J|A|C|S ARTICLES

Published on Web 02/22/2010

Phospholipid Encapsulated Semiconducting Polymer Nanoparticles: Their Use in Cell Imaging and Protein Attachment

Philip Howes,[†] Mark Green,*[,†] James Levitt,[†] Klaus Suhling,[†] and Mary Hughes[‡]

Department of Physics, King's College London, Strand, London WC2R 2LS, U.K. and School of Biomedical & Health Sciences, King's College London, Franklin-Wilkins Building, Stamford Street, London SE1 9NH, U.K.

Received January 10, 2010; E-mail: mark.a.green@kcl.ac.uk

Abstract: Semiconducting polymer nanospheres (SPNs) have been synthesized and encapsulated in phospholipid micelles by a solvent evaporation technique. Four different conjugated polymers were used, yielding aqueous dispersions of nanoparticles which emit across the visible spectrum. The synthesis was simple and easily reproducible, and the resultant nanoparticle solutions exhibited high colloidal stability. As these encapsulated SPNs do not contain any toxic materials and show favorable optical properties, they appear to be a promising imaging agent in biomedical and imaging applications. The SPNs were used in simple fluorescence imaging experiments and showed uptake in SH-SY5Y neuroblastoma and live HeLa cells. Carboxylic acid functionalized SPNs were also synthesized and conjugated to bovine serum albumin (BSA) by carbodiimide-mediated chemistry, a key step in the realization of targeted imaging using conjugated polymers.

Introduction

The use of nanomaterials in biological sciences is widespread, where they have proven to be vital tools in a diverse range of applications from drug delivery in vivo to sensitive biosensors in vitro. This area of science has received much interest in the last couple of decades, and research in the field is ever increasing with new types of materials and applications being continually discovered. The nanomaterials of interest possess unique physical and chemical properties, such as superparamagnetism or stable fluorescence, which lend them to biological applications. Within the field of fluorescence-based studies, quantum dots have received a great deal of interest due to their bright and stable fluorescence. They have narrow and size-dependent emission lines with a considerable Stokes shift and broad absorption bands such that multiple excitation sources are not required for different quantum dot types and sizes. They have high fluorescence brightness, are resistant to photobleaching, and can be functionalized with a range of surfactants and biomolecules.[1−5] Colloidal stability, particle aggregation, and nonselective adsorption have traditionally been problems but progress has been made recently in circumventing these issues.

A particularly exciting application of fluorescent nanoparticles will be for in vivo imaging. This has long been heralded as a potential revolution in disease diagnostics, especially in cancer diagnosis and management.[6,7] It is envisaged that nanoparticle systems will be used for monitoring predictive molecular changes to prevent precancerous cells from becoming malignant, for imaging cancer in its presymptomatic stages, and as an efficient means of detecting and treating established cancerous cells.[7] Despite their promise, the suitability of quantum dots as biolabeling agents in this context is questionable as most contain highly toxic materials (e.g., cadmium). There have been mixed results in toxicity studies of quantum dots. In some studies, no short-term toxicity has been observed in cells[8] or in live animals.[9,10] Contradictory studies have found that quantum dot cores can damage DNA and be acutely toxic to cells.[11−14] Biocompatibility and aqueous stability can be increased with the addition of relatively benign inorganic shells and encapsulation layers,[15] but this leads to an unwanted increase in hydrodynamic radius. Recent studies have reduced problems with excessive hydrodynamic radii,[15] but problems persist with

[†] Department of Physics.
[‡] School of Biomedical & Health Sciences.

(1) Jaiswal, J. K.; Simon, S. M. *Trends Cell Biol.* **2004**, *14*, 497–504.
(2) Alivisatos, A. P.; Gu, W. W.; Larabell, C. *Annu. Rev. Biomed. Eng.* **2005**, *7*, 55–76.
(3) Parak, W. J.; Pellegrino, T.; Plank, C. *Nanotechnology* **2005**, *16*, R9–R25.
(4) Ballou, B.; Lagerholm, B. C.; Ernst, L. A.; Bruchez, M. P.; Waggoner, A. S. *Bioconjugate Chem.* **2004**, *15*, 79–86.
(5) De, M.; Ghosh, P. S.; Rotello, V. M. *Adv. Mater.* **2008**, *20*, 4225–4241.
(6) Bertolini, G.; Paleari, L.; Catassi, A.; Roz, L.; Cesario, A.; Sozzi, G.; Russo, P. *Curr. Pharm. Anal.* **2008**, *4*, 197–205.
(7) Cai, W. B.; Hsu, A. R.; Li, Z. B.; Chen, X. Y. *Nanoscale Res. Lett.* **2007**, *2*, 265–281.
(8) Jaiswal, J. K.; Mattoussi, H.; Mauro, J. M.; Simon, S. M. *Nat. Biotechnol.* **2003**, *21*, 47–51.
(9) Larson, D. R.; Zipfel, W. R.; Williams, R. M.; Clark, S. W.; Bruchez, M. P.; Wise, F. W.; Webb, W. W. *Science* **2003**, *300*, 1434–1436.
(10) Kim, S.; Lim, Y. T.; Soltesz, E. G.; De Grand, A. M.; Lee, J.; Nakayama, A.; Parker, J. A.; Mihaljevic, T.; Laurence, R. G.; Dor, D. M.; Cohn, L. H.; Bawendi, M. G.; Frangioni, J. V. *Nat. Biotechnol.* **2004**, *22*, 93–97.
(11) Derfus, A. M.; Chan, W. C. W.; Bhatia, S. N. *Nano Lett.* **2004**, *4*, 11–18.
(12) Hoshino, A.; Fujioka, K.; Oku, T.; Suga, M.; Sasaki, Y. F.; Ohta, T.; Yasuhara, M.; Suzuki, K.; Yamamoto, K. *Nano Lett.* **2004**, *4*, 2163–2169.
(13) Liang, J. G.; He, Z. K.; Zhang, S. S.; Huang, S.; Ai, X. P.; Yang, H. X.; Han, H. Y. *Talanta* **2007**, *71*, 1675–1678.
(14) Anas, A.; Akita, H.; Harashima, H.; Itoh, T.; Ishikawa, M.; Biju, V. *J. Phys. Chem. B* **2008**, *112*, 10005–10011.

unstable emissive properties like blinking and low emission rates.[16] Regardless of fluorescence properties, long-term toxicity will always be a real concern, and it is important that alternative materials are studied.[7,17] Current alternatives include dye-doped silica nanospheres[18] and organic fluorophores and dyes;[19] however, these materials also have their own associated problems, such as low-photobleaching thresholds.

In this work, luminescent conjugated polymers were used in the synthesis of fluorescent nanoparticles which were attached to a protein with no detrimental effects and used in imaging experiments. These polymers are organic semiconductors which possess the ease of processing of plastics and the electronic behavior of metals and semiconductors and are well understood due to their application in light-emitting devices.[20] They have found application in a variety of fields because of their bright photo- and electroluminescence. The conjugated backbone gives rise to π-electron delocalization and a band structure, and the $\pi-\pi^*$ electronic transition allows exciton formation which facilitates luminescence.[21] They are considered as potentially useful in the production of nanoparticles for use in fluorescence imaging as they have high quantum yields and extinction coefficients in solution and, therefore, exhibit high fluorescence brightness.[22−24] Importantly, they are relatively benign and should overcome the potential toxicity problems associated with quantum dots.[11−14]

Various groups have examined semiconducting polymers as potential biological probes. The use of simple conjugated polymers which have been functionalized with side chains to impart water solubility and allow bioconjugation are rare, and most alterations to the conjugated polymer structure resulted in quenched emission. Heeger suggested that convenient polymers such as the PPV family of materials are potentially useful if a side group (usually ionic) is added to induce solubility in water.[25] In the seminal cases of using light-emitting polymers as biological probes, the *quenching* of emission was used as the indicator of biological activity, and hence, biological material was not imaged using the polymer's emissive properties.[26] The chemistry utilized was relatively difficult and specific and did not use readily available polymers, negating the potentially vast color library supplied by the large number of existing conjugated polymers already commercially available. Similar work was reported using specifically designed and synthesized polyelectrolytes, which showed enhanced emission when bound to a specific protein.[27,28] Nonspecific binding was also observed in some cases, as well as emission quenching. In all cases, the conjugated polymer has to be chemically modified to be used in water, and usually, the polymers were *not* used as *biological labels*; *sensing* was achieved in solution by observing the effect of biological entities on the photoluminescence, and hence, the term biosensor is more appropriate. Recently, this phenomenon, termed "superquenching" of PPV-related materials, has been reported as a key labeling technology.[29]

Swager has also carried out extensive work using conjugated polymers for biological applications. In these cases, again, the polymers have been chemically functionalized to add a relevant side group; hence, the process is not readily available to nonchemists such as biology-trained imaging scientists. For example, polymeric materials have been used as oxygen sensors,[30] and glycoside functionalized polymers have been used to detect bacteria.[31]

Conjugated polymers with ionic side groups (normally cationic, although anionic species have also been used) have been have been used extensively in DNA assays,[32−40] again using the changing optics to sense interactions with biological materials. These sensing applications are different from typical labeling, as the biological material is not imaged and any data acquired is based on the alteration of the polymer optics, notably shifts in the emission or absorption intensity or spectral position. Specific examples include a carboxylate modified polymer which has been linked to peptides with an emission quenching group.[41] The hydrolysis of peptides was monitored and the photoluminescence enhancement monitored after the quenching group was removed. Other polymers have been modified to effect water solubility, although no labeling studies have been reported.[42] Notably, a nonionic approach has also been developed to producing a water-soluble conjugated polymer by grafting on hydroxyl side groups.[43] Unfortunately, the new side group quenches the emission quantum yield, and as far as we are aware, to date, the material has not been used in biological labeling or sensing.

To the best of our knowledge, there is one report where a functionalized conducting polymer was used to label bacteria.[44]

(15) Liu, W.; Howarth, M.; Greytak, A. B.; Zheng, Y.; Nocera, D. G.; Ting, A. Y.; Bawendi, M. G. *J. Am. Chem. Soc.* **2008**, *130*, 1274–1284.
(16) Yao, J.; Larson, D. R.; Vishwasrao, H. D.; Zipfel, W. R.; Webb, W. W. *Proc. Natl. Acad. Sci. U.S.A.* **2005**, *102*, 14284–14289.
(17) Choi, H. S.; Liu, W.; Misra, P.; Tanaka, E.; Zimmer, J. P.; Ipe, B. I.; Bawendi, M. G.; Frangioni, J. V. *Nat. Biotechnol.* **2007**, *25*, 1165–1170.
(18) Yan, J. L.; Estevez, M. C.; Smith, J. E.; Wang, K. M.; He, X. X.; Wang, L.; Tan, W. H. *Nano Today* **2007**, *2*, 44–50.
(19) Miyawaki, A.; Sawano, A.; Kogure, T. *Nat. Rev. Mol. Cell. Biol.* **2003**; S1−S7.
(20) Dini, D. *Chem. Mater.* **2005**, *17*, 1933–1945.
(21) Schwartz, B. J. *Annu. Rev. Phys. Chem.* **2003**, *54*, 141–172.
(22) Wu, C. F.; Szymanski, C.; McNeill, J. *Langmuir* **2006**, *22*, 2956–2960.
(23) Wu, C. F.; Szymanski, C.; Cain, Z.; McNeill, J. *J. Am. Chem. Soc.* **2007**, *129*, 12904-+.
(24) Wu, C.; Bull, B.; Szymanski, C.; Christensen, K.; McNeill, J. *ACS Nano* **2008**, *2*, 2415–2423.
(25) Oikawa, H.; Oshikiri, T.; Kasai, H.; Okada, S.; Tripathy, S. K.; Nakanishi, H. *Polym. Advan. Technol.* **2000**, *11*, 783–790.
(26) Landfester, K.; Montenegro, R.; Scherf, U.; Guntner, R.; Asawapirom, U.; Patil, S.; Neher, D.; Kietzke, T. *Adv. Mater.* **2002**, *14*, 651–655.
(27) Landfester, K. *Annu. Rev. Mater. Res.* **2006**, *36*, 231–279.
(28) Howes, P.; Thorogate, R.; Green, M.; Jickells, S.; Daniel, B. *Chem. Commun.* **2009**, 2490–2492.
(29) Wu, M.; Yang, G.; Wang, M.; Wang, W.; Wang, M.; Liu, T. *Chem. Res. Chin. U.* **2008**, *24*, 653–657.
(30) Piok, T.; Gadermaier, C.; Wenzl, F. P.; Patil, S.; Montenegro, R.; Landfester, K.; Lanzani, G.; Cerullo, G.; Scherf, U.; List, E. J. W. *Chem. Phys. Lett.* **2004**, *389*, 7–13.
(31) Zalipsky, S. *Adv. Drug Deliver. Rev.* **1995**, *16*, 157–182.
(32) Caliceti, P.; Veronese, F. M. *Adv. Drug Delivery Rev.* **2003**, *55*, 1261–1277.
(33) Fruijtier-Pölloth, C. *Toxicology* **2005**, *214*, 1–38.
(34) Prentice, D. E.; Majeed, S. K. *Toxicol. Lett.* **1978**, *2*, 119–122.
(35) Vakil, R.; Kwon, G. S. *Langmuir* **2006**, *22*, 9723–9729.
(36) Adlakha-Hutcheon, G.; Bally, M. B.; Shew, C. R.; Madden, T. D. *Nat. Biotechnol.* **1999**, *17*, 775–779.
(37) Working, P. K.; Newman, M. S.; Sullivan, T.; Yarrington, J. *J. Pharmacol. Exp. Ther.* **1999**, *289*, 1128–1133.
(38) Johnsson, M.; Hansson, P.; Edwards, K. *J. Phys. Chem. B* **2001**, *105*, 8420–8430.
(39) Dubertret, B.; Skourides, P.; Norris, D. J.; Noireaux, V.; Brivanlou, A. H.; Libchaber, A. *Science* **2002**, *298*, 1759–1762.
(40) Depalo, N.; Mallardi, A.; Comparelli, R.; Striccoli, M.; Agostiano, A.; Curri, M. L. *J. Colloid Interface Sci.* **2008**, *325*, 558–566.
(41) Erogbogbo, F.; Yong, K.-T.; Roy, I.; Xu, G.; Prasad, P. N.; Swihart, M. T. *ACS Nano* **2008**, *2*, 873–878.
(42) Nguyen, T. Q.; Doan, V.; Schwartz, B. J. *J. Chem. Phys.* **1999**, *110*, 4068–4078.
(43) Traiphol, R.; Charoenthai, N.; Srikhirin, T.; Kerdcharoen, T.; Osotchan, T.; Maturos, T. *Polymer* **2007**, *48*, 813–826.

In this case, the side groups of the polymer were modified to allow labeling, although the aim of the report was not the labeling ability; in this case, the biocidal activity of the polymer was being investigated.

In these systems, the introduction of the required functional group appears, in the majority of cases, to result in alterations with the emission sensitivity or other optical characteristics. Ideally, a simple conjugated polymer with known optics would be preferred without the need to introduce side groups that may change the polymer optics or the need to design new polymers with the required properties, a lengthy and difficult process. Simple available semiconducting polymers, such as MEH−PPV, would be ideal, as the material has been investigated in depth and is commercially available. As it stands, MEH−PPV and similar off-the-shelf polymers have excellent optical properties, potentially useful for labeling, but do not possess the required linking groups for bioconjugation or water solubilization. This does at first sound contradictory, as the introduction of side groups to allow conjugation results in a negative impact on the polymer optics, as described above. We therefore require a system where MEH−-PPV (and other convenient polymers) are transferred to water without the alteration of the polymer, and ideally, we also desire the potential to link to biological entities, such as proteins, antibodies, etc. We cannot have both (or either) using just the polymer system.

Semiconducting polymer nanospheres (SPNs) have been synthesized by two main routes, notably by the McNeill group.[22−24] The reprecipitation method takes advantage of the conformational change brought about by introduction of the hydrophobic polymer into an aqueous environment.[25] However, conjugated polymer nanospheres produced in this fashion do not always have a surfactant, which limits the possibility of bioconjugation.[23,24] Silica encapsulation has been performed, which potentially addresses this problem.[22] Another method of synthesis is by miniemulsion.[26−28] In this method, nanoparticles are formed in cavitation bubbles produced by shearing an emulsion system with ultrasound. The solution contains a surfactant to bestow water solubility upon the polymer. When the solvent evaporates from the bubbles containing the polymer, stable nanoparticles are formed. However, these methods can be quite low yield, and prolonged use of ultrasound can cause degradation of the polymer chains.[29] It has been demonstrated that SPNs show favorable properties for use in bioimaging. These include fast radiative rates, high photostability, high fluorescence brightness, large two-photon action cross sections, ease of processing and low cellular toxicity.[23,24,27,28,30]

Throughout the previously reported routes to conjugated polymer nanoparticles, a simple engineered surface species which is biocompatible, such as poly(ethylene glycol) (PEG), and provides the option for further conjugation to a wide range of biological molecules without compromising the emitting species is highly desirable yet is not readily available. PEGs have been used extensively in clinical applications.[31] PEG-capped nanoparticles show increased circulation times in vivo due to decreased detection and clearance from the body by the reticuloendothelial system (RES).[32] Importantly, they exhibit low toxicity.[33,34] PEGs can be attached to phospholipids to produce amphiphilic molecules which form micelle structures in solution which allows the incorporation of further linking groups or biological molecules such as DNA.[35] An important application of PEG−phospholipids has been their use in controlling drug circulation and release in vivo.[36−38] One of the major factors in producing biocompatible nanoparticles for biological applications is water solubility. The main categories of nanoparticles with applications in this field, quantum dots or magnetite nanoparticles, for example, tend to be insoluble in water and require some kind of phase-transfer treatment. PEG−phospholipids have been used for this.[39,40] Encapsulation in phospholipid micelles bestows favorable biocompatibility properties upon the encapsulated particles,[41] and they are known to have low critical micelle concentrations and high kinetic stabilities.[38,41] Charged phospholipids experience repulsive forces between micelles, which is useful in decreasing aggregation, and the polymeric corona of PEG introduces a steric repulsion component.[38] Importantly, PEG content and chain length can be tailored to the requirements of the application.[39] Phosphatidycholine is often used in conjunction with PEG−phospholipids to control the density of packing of the PEG chains on the particle surface. 1,2-Diacyl-*sn*-glycero-3-phosphoethanolamine−*N*-[methoxy(polyethylene glycol)-2000] (PEG_{2000}−PE) and 1,2-dipalmitoyl-*sn*-glycero-3-phosphocholine (DPPC) were used in the current study with reference to work performed on quantum dot encapsulation.[39]

In this paper, a high-yield synthesis of SPNs is presented. The nanoparticles were formed in PEG_{2000}-PE/DPPC micelles by solvent evaporation under high shear. Encapsulation in micelles is normally performed on preformed hydrophobic nanoparticles, but in this synthesis micellar encapsulation was an intrinsic part of particle formation. This synthesis resulted in highly stable aqueous dispersion of SPNs. Uptake of red-emitting SPNs was observed in simple fluorescence imaging experiments using fixed SH-SY5Y neuroblastoma and live HeLa cells. Finally, carboxylic acid functionalized PEG−PE was used to functionalize the SPNs and facilitate conjugation with bovine serum albumin (BSA).

Materials and Methods

Four conjugated polymers were studied in this work. Poly[2,5-di(3′,7′-dimethyloctyl)phenylene-1,4-ethynylene] (PPE, MW unknown), poly[2-(2′,5′-bis(2′′-ethylhexyloxy)phenyl)-1,4-phenylenevinylene] (BEHP−PPV, MW 30000 minimum), poly[(9,9-di-*n*-octylfluorenyl-2,7-diyl)-*alt*-(benzo[2.1.3]thiadiazol-4,8-diyl)] (PF, MW 5−8000), and poly[2-methoxy-5-(2-ethylhexyloxy)-1,4-phenylenevinylene] (MEH−PPV, MW 40−70000). All polymers were dissolved in dichloromethane (DCM) prior to use. All were obtained from Sigma-Aldrich. 1,2-Diacyl-*sn*-glycero-3-phosphoethanolamine−*N*-[methoxy(polyethylene glycol)-2000] (PEG_{2000}−PE) and 1,2-dipalmitoyl-*sn*-glycero-3-phosphocholine (DPPC) were purchased from Avanti Lipids. *N*-(3-Dimethylaminopropyl)-*N*′-ethylcarbodiimide hydrochloride (EDC), phosphate-buffered saline pH 7.4 (PBS), bovine serum albumin (BSA), and tris(hydroxymethyl)aminomethane hydrochloride (Tris-HCl) were obtained from Sigma-Aldrich. All chemicals were used as received.

In a typical synthesis, 0.85 mg of conjugated polymer was added to 16 mL of dichloromethane (DCM) and stirred for 2 days to ensure complete dissolution. The polymer solution was filtered through a 0.2 μm membrane filter prior to addition of 7 mg of PEG_{2000}−PE and 3 mg of DPPC. The solution was stirred for a further 10 min and then added to 20 mL of water under sonication. After 1 min, the solution was stirred rapidly while under sonication. After 5 min, the solution became clear and was immediately filtered through filter paper. The reaction solution was then centrifuged for 30 min, and the solid collected was discarded.

For conjugation of MEH−PPV micelles with bovine serum albumin (BSA), the synthesis of carboxylic acid functionalized was

(44) Nguyen, T. Q.; Martini, I. B.; Liu, J.; Schwartz, B. J. *J. Phys. Chem. B* **2000**, *104*, 237–255.

performed as the standard synthesis, except 2 mg of PEG_{2000}−PE carboxylic, 5 mg of PEG_{2000}−PE, and 3 mg of DPPC was used. Conjugation with BSA was performed by linking the carboxylic acid groups on the SPNs with an amine group on the BSA. Eight milligrams of sulfo-NHS, 60 mg of EDC, and 8 mg of BSA were separately added to 2 mL of PBS pH 7.4 each. All solutions were stirred for 2 h to ensure complete dissolution. The sulfo-NHS, EDC, and BSA PDS solutions were all added to 2 mL of the carboxylic acid functionalized SPNs to make an 8 mL reaction solution and stirred for 2 h. A 0.25 g tablet of Tris-HCl buffer was then added to quench the reaction.

Transmission electron microscopy (TEM) was performed on an FEI Tecnai 20 at 200 kV for high-resolution imaging. Samples were drop cast and dried on carbon film copper grids. Absorption spectroscopy was performed on a Perkin-Elmer Lambda 800 UV/vis spectrometer, and emission spectra were collected on a Perkin-Elmer LS50B emission spectrometer. Dynamic light scattering (DLS) was used to obtain mean hydrodynamic diameters of the samples. This was performed on a Delsa Nano C particle analyzer.

Quantum yields were measured by comparison with fluorescence standards. Atto 390 (PPE and BEHP−PPV), fluoroscein (PF), and rhodamine 6G (MEH−PPV) were used. The extinction coefficients were calculated using the Beer−Lambert law by varying the concentration of the polymers in DCM and recording the absorption peaks.

SHSY5Y neuroblastoma cells were maintained in DMEM supplemented with 10% fetal bovine serum (FBS) 2 mM glutamine. Cells were seeded onto glass coverslips 24 h prior to experimentation. Cells were treated with a 1:10 dilution of MEH−PPV SPNs in 500 μL of Optimem containing 10% FBS, 2 mM glutamine, and antimicrobials for 18 h. Cells were washed twice in phosphate buffered saline (PBS) and fixed in 3.7% paraformalde in PBS. Cells were permeabilized with 0.4% triton in PBS supplemented with 1% sucrose. The cells were then incubated with Alexa Fluor phalloidin (Invitrogen) and mounted using Vectasheild mounting medium containing 4′,6-diamidino-2-phenylindole. Visualization was carried out using a Leica DMIRE2 confocal microscope equipped with an LED diode laser to excite DAPI at 405 nm. The emission wavelength range chosen was 419−470 nm. The Alexa Fluor 488 conjugate and the nanoparticles were excited using an argon laser at 488 nm (and an emission range of 515−550 nm and 654−810 nm, respectively). Visualization was carried out on the inverted samples, using a Leica HCX PL APO 63x oil immersion lens with a numerical aperture of 1.4 and a pinhole size equivalent to 1 Airy band resolution. An overlay was created using the Image J software package (http://rsbweb.nih.gov/ij/).

HeLa cells were cultured in Dulbecco's Modified Eagles Medium (DMEM). Following incubation with the conjugated polymer nanoparticles for 18 h at 37 °C in a 5% CO_2 environment, the cells were washed twice with clear, nonfluorescent imaging medium (DMEM). The live HeLa cells were kept at 37 °C for imaging by use of a heated six-well plate (SmartSlide-6TM microincubator) as part of a microincubation system (WaferGen Biosystems SmartSlideTM 50). Confocal fluorescence imaging was performed using an inverted Leica TCS SP2 scanning laser confocal microscope. Images were acquired using 488 nm excitation from an Ar^+ laser using a 63× water immersion objective (NA = 1.2). The emitted fluorescence was collected through the same objective before being directed through the descanning port of the microscope through a pinhole onto a photomultiplier detector. The detection wavelength was set to 600 ± 20 nm, and the line scan speed for imaging was 400 Hz. Brightfield transmitted light and reflected fluorescence images were collected simultaneously.

Results and Discussion

The SPNs in this study were formed by direct encapsulation of hydrophobic materials in micelles. The proposed reaction mechanism is as follows. The conjugated polymer was mixed with the PEG_{2000}−PE and DPPC in dichloromethane (DCM) until complete dissolution of all solids had occurred. This solution was added to water under sonication which induced cavitation and droplet formation of the DCM/polymer solution. Rapid stirring increased the shear in the system and the evaporation rate of the DCM. The phospholipids oriented themselves such that the hydrophilic ends transferred to the water, while the hydrophobic acyl chains stayed in the DCM droplets, forming DCM solution filled micelles. However, as the DCM began to evaporate it would leave the micelles, causing them to shrink. During this process the hydrophobic polymer was trapped and compressed inside the micelle, forming the nanoparticle cores. The result was a stable dispersion of phospholipid encapsulated conjugated polymer nanoparticles in water. It should be pointed out that nanoparticle formation by reprecipitation from DCM into water is possible but occurs at an extremely low yield under the conditions used, so it is expected that the only way that such a high yield of SPNs can occur is by micellar encapsulation. This is supported by the fact that the SPNs are stable in water for long periods (months) and low aggregation rates are observed, as would be expected from PEG-phospholipid encapsulated nanoparticles.

Four conjugated polymers were studied in this work: poly[2,5-bis(3′,7′-dimethyloctyl)phenylene-1,4-ethynylene] (referred to as PPE), poly[2-(2′,5′-bis(2′′-ethylhexyloxy)phenyl)-1,4-phenylenevinylene] (BEHP−PPV), poly[(9,9-di-*n*-octylfluorenyl-2,7-diyl)-*alt*-(benzo[2,1,3]thiadiazol-4,8-diyl)] (PF), and poly[2-methoxy-5-(2-ethylhexyloxy)-1,4-phenylenevinylene](MEH−PPV). Parts A and B of Figure 1 show the optical characterization of all four conjugated polymers as SPN solutions in water. It is seen that the emission wavelengths range across the visible spectrum, from blue (418 nm) to red (593 nm), demonstrating the versatility of using conjugated polymers. Unlike quantum dots, the color of emission of SPNs is not dependent upon nanoparticle size but on chemical composition of the conjugated polymer. This means that a narrow size distribution is not imperative in obtaining narrow emission lines, which gives some leeway in the synthesis methodology. The absorption spectra are reasonably wide, such that all solutions can be excited with a single source (e.g., 365 nm UV lamp), although tuning the excitation energy to the individual polymers will obviously maximize fluorescence brightness. Figure 1C shows the SPN solutions in ambient light, and under UV excitation (365 nm). The solutions are transparent and colored and exhibit strong fluorescence under UV.

The optical characteristics of the parent polymers in DCM differed from those of the SPNs in water. The MEH−PPV, BEHP−PPV, and PF SPNs all exhibited a red shift in their absorption and emission. This was attributed the change in spatial environment of the polymer, similar to previous reports on conjugated polymers in solutions and thin films, where a reduction in the average conjugation length occurs due to chain confinement.[42−44] The SPN absorption spectra of these polymers were broader than those of the parent polymers in DCM. This was attributed to a broadening of the conjugation length distribution of the conjugated polymer chain segments which occurred because of coiling and twisting of the chains during nanoparticle formation. All of the different lengths of chromophore absorb energy, so a wider absorption spectrum was obtained which enveloped all of the absorption bands, with a net shift into the red.[45] The observed red shift in the emission

(45) Traiphol, R.; Sanguansat, P.; Srikhirin, T.; Kerdcharoen, T.; Osotchan, T. *Macromolecules* **2006**, *39*, 1165–1172.

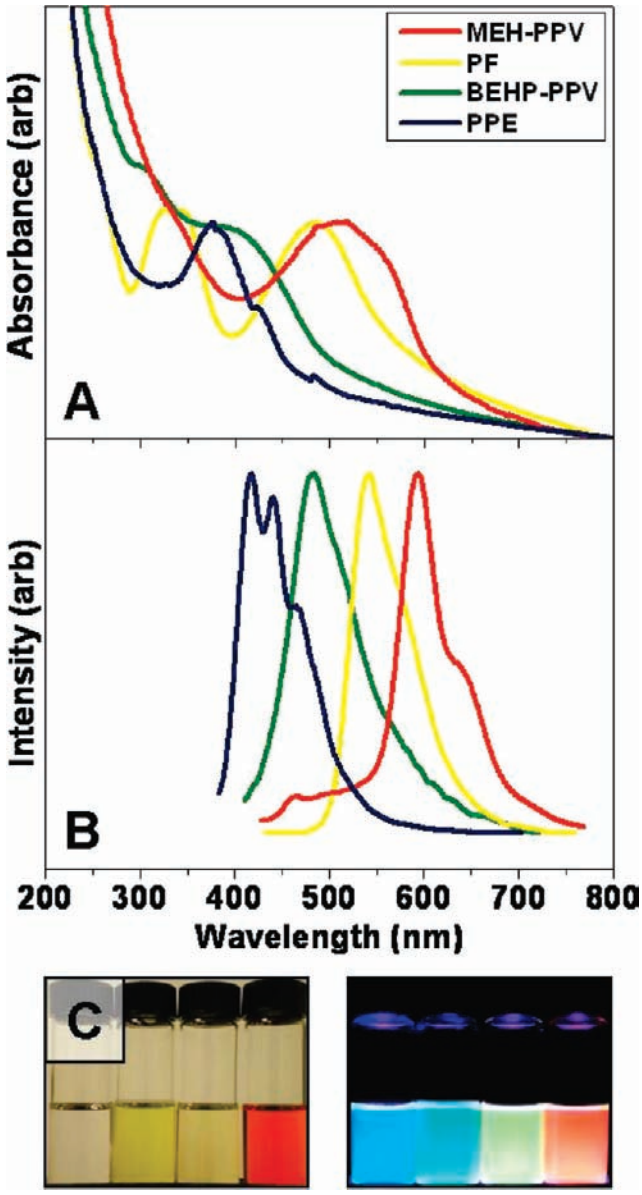

Figure 1. Normalized absorption (A) and emission (B) spectra of all four SPNs types. Part C shows the clear aqueous SPN solutions and the same solutions under UV excitation.

of MEH−PPV, BEHP−PPV, and PF was likely due to aggregation of polymer chains, causing π-orbital overlap, delocalization of the π-electrons across several chains, and a reduction in bandgap energy.[21] There was a lower energy shoulder on both the MEH−PPV and the BEHP−PPV emission spectra. This corresponded to relaxation of π-electrons through a ground state energy level.[44] The emission was relatively narrow for all SPNs because of the migration of energy states along the polymer chain to the lowest energy segments, which then emit.[46] The change in optical behavior between the DCM and SPN solution was particularly pronounced in MEH−PPV. Figure 2 shows the full optical characterization of MEH−PPV in DCM and in an aqueous SPN solution. A red shift of 37 nm was seen in the emission spectrum, and a redshift of 5 nm was seen in the absorption peak.

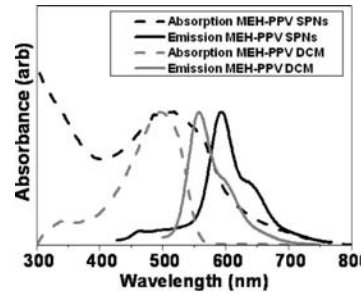

Figure 2. Comparison of emission and absorption spectra of MEH−PPV in DCM with MEH−PPV SPNs in water.

Table 1. Analysis of All Four Polymer SPNs in Water

	PPE	BEHP−PPV	PF	MEH−PPV
TEM diameter (mean) (nm)	71.05	59.63	71.30	74.30
standard deviation	18.02	19.58	30.86	26.25
DLS diameter (mean) (nm)	91.56	80.06	101.10	93.43
polydispersity index	0.17	0.14	0.19	0.26
emission peak (nm)	418	484	542	593
quantum yield (%)	18.98	1.26	26.9	1.3
extinction coefficient (L/g cm)	56.5	9.9	59.8	85.0
extinction coefficient (M^{-1} cm)		297000	299000	3825000

The PPE SPNs exhibited different optical behavior to the other polymers. There was a 5 nm blue shift in the absorption and the emission. PPE conjugated polymers exhibit complex phase and packing behavior in the solid state.[24] This is partly due to the ethynylene linkages (C−C triple bonds) along its backbone which severely restrict rotational freedom of the polymer chain. This strengthens the structure and encourages the polymer to form ordered arrays as a solid.[47] The introduction of C−C triple bonds into polymer chains has the effect of shortening the conjugation length, which is why PPEs exhibit high energy emission.[48]

Table 1 shows the quantum yields of the SPN solutions, measured relative to fluorescence standards. The largest quantum yield was observed from the PF SPNs at 26.9% and the smallest from BEH−PPV at 1.26%. This spread in quantum yields for different polymers is consistent with previous reports.[24] The quantum yield of a particular conjugated polymer is dependent on its structure, and how the chains pack together when they are confined in the nanoparticle. Generally, a drop in quantum yield is seen when a polymer chain moves from free in solution to confinement in a solid. This is because of an increased number of structural defects occurring due to conformational changes brought on by chain confinement. Nonradiative decay to the ground state can occur when excitons migrate to such defects.[49] Increased overlap of π-orbitals can result in the formation of new electronic species, such as excimers and aggregates, which quench emission.[21] In our study, the PPV polymers showed a substantially lower quantum yield than the PF and PPE. Both the PPE and PF polymers form more ordered structures in the solid state than PPV.[47,50] Attachment of long side chains to conjugated polymers increases the separation of neighboring chains and thus decreases the occurrence of emission-quenching

(46) Padmanaban, G.; Ramakrishnan, S. *J. Am. Chem. Soc.* **2000**, *122*, 2244–2251.
(47) Jiang, X. M.; Wu, C. C.; Wohlgenannt, M.; Huang, W. Y.; Kwei, T. K.; Okamoto, Y.; Vardeny, Z. V. *Phys. B* **2003**, *338*, 235–239.
(48) Hirohata, M.; Tada, K.; Kawai, T.; Onoda, M.; Yoshino, K. *Synth. Met.* **1997**, *85*, 1273–1274.
(49) Johansson, D. M.; Theander, M.; Srdanov, G.; Yu, G.; Inganas, O.; Andersson, M. R. *Macromolecules* **2001**, *34*, 3716–3719.
(50) Scherf, U.; List, E. J. W. *Adv. Mater.* **2002**, *14*, 477-+.

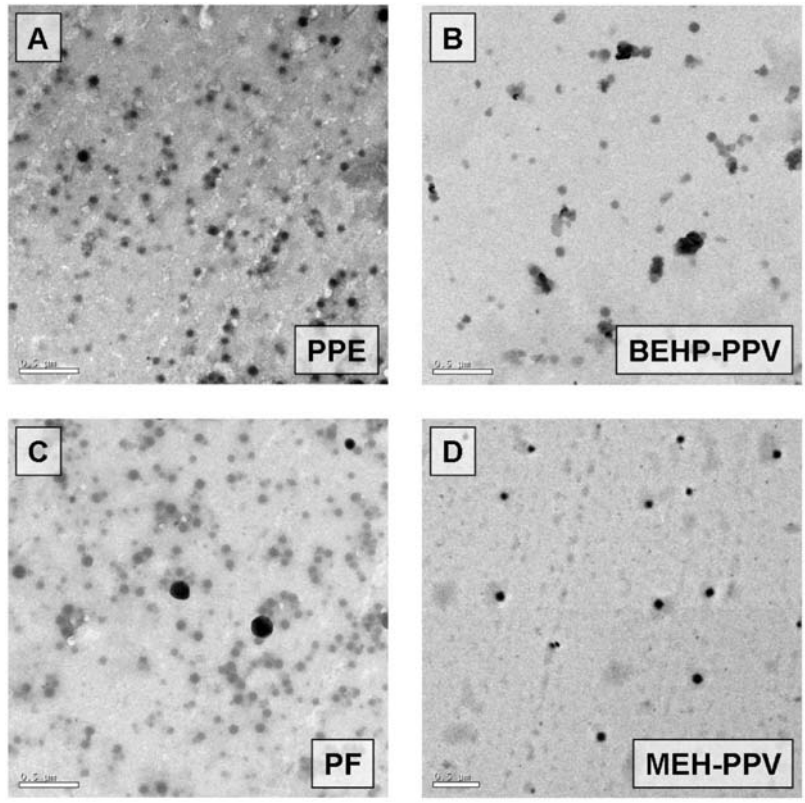

Figure 3. Transmission electron micrographs of PPE (A), BEHP−PPV (B), PF (C), and MEH−PPV (D) SPNs. Scale bar 500 nm.

interchain species.[48] The above factors contributed substantially toward the disparity in quantum yields between the polymers.

Table 1 also shows the extinction coefficients of all polymers in DCM. Conjugated polymers are characterized by high extinction coefficients, and it is the combination of quantum yield and extinction coefficient which gives the high fluorescence brightness. It is important to note that these extinction coefficients compare extremely well with those of quantum dots. For CdSe quantum dots the extinction coefficients have been measured, ranging between 1 and 3 L/g cm (depending on molecular weight of the quantum dot), whereas the conjugated polymers used in this study range from 9.9 to 85.0 L/g cm.[51] In our previous work, we have used BEHP−PPV nanospheres for cellular imaging where they exhibited strong and stable fluorescence.[28] Given that the BEHP−PPV SPNs produced in the current work have the lowest extinction coefficient and quantum yield of the four polymers used, it is expected that the other polymers will exhibit very strong fluorescent brightness, sufficient for demanding fluorescence applications.

We also measured the mean diameters of the SPNs measured by dynamic light scattering (DLS) and transmission electron microscopy (TEM) (Table 1). The DLS measurement gave the mean hydrodynamic diameter of the SPNs in water and the measurements taken from the TEM gave the diameter of the conjugated polymer core. For three of the polymers (PPE, BEHP−PPV, and MEH−PPV) the difference between the hydrodynamic diameter and the core diameter of the SPNs was ca. 20 nm. The PF SPNs showed a ca. 30 nm difference. It is expected that this difference in diameter can be attributed to the presence of the PEG-phospholipids on the surface of the nanoparticles. This relatively small difference between the DLS and TEM diameters also suggested that there was a low degree of aggregation in the SPN solution. Figure 3 shows the transmission electron micrographs of the four different SPN samples. These clearly illustrate the formation of nanoparticles in each case.

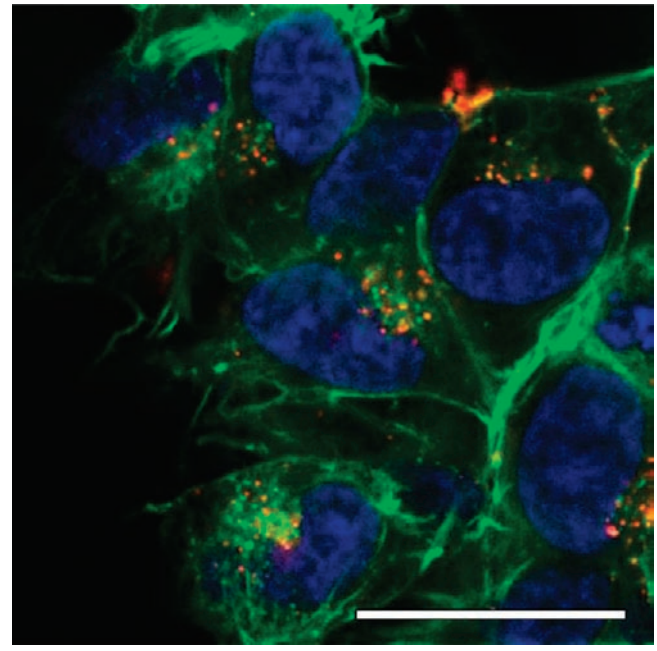

Figure 4. Confocal microscope image of SH-SY5Y neuroblastoma cells treated with MEH−PPV SPNs for 18 h. The SPNs are seen to cluster in the perinuclear region within the cells, suggesting they are in vesicles. The scale bar represents 25 μm.

(51) Striolo, A.; Ward, J.; Prausnitz, J. M.; Parak, W. J.; Zanchet, D.; Gerion, D.; Milliron, D.; Alivisatos, A. P. *J. Phys. Chem. B* **2002**, *106*, 5500–5505.

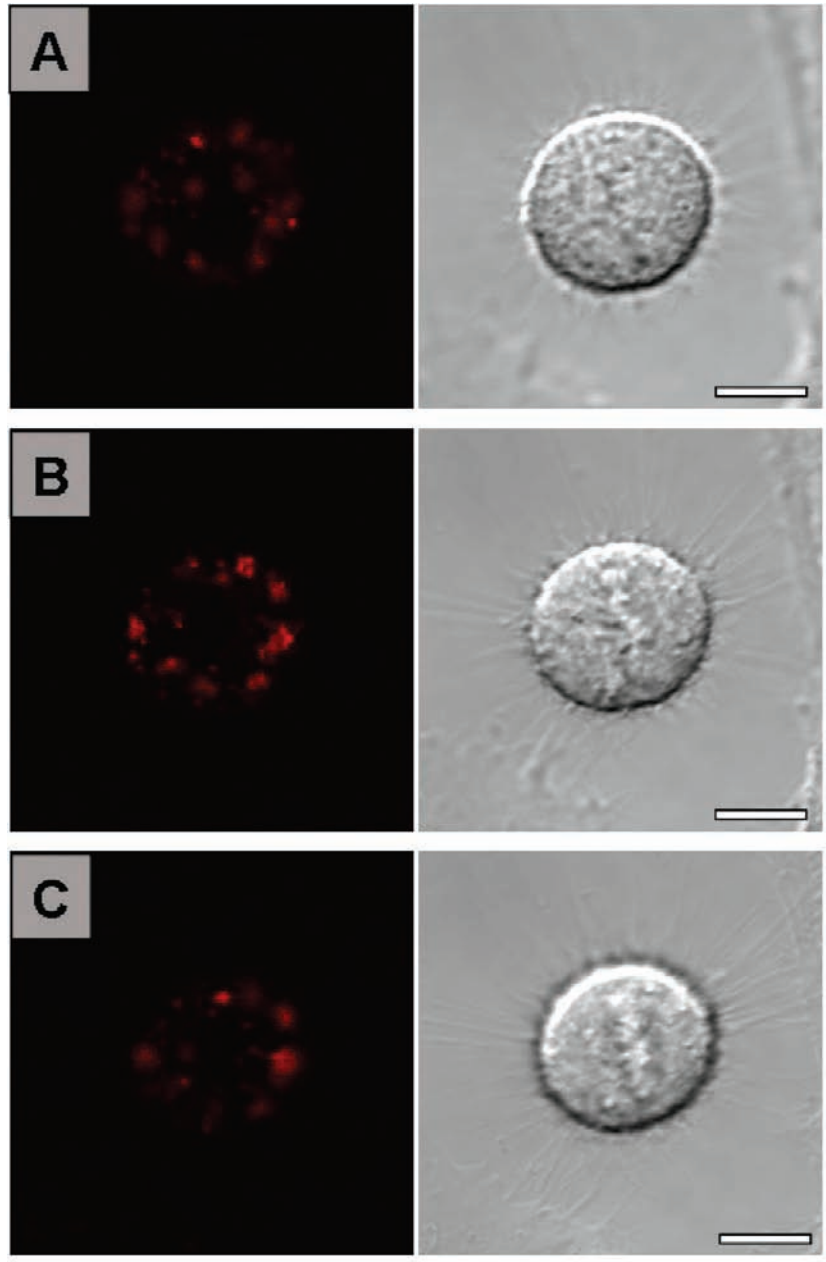

Figure 5. Confocal fluorescence (left) and brightfield (right) images of a HeLa cell incubated with the SPNs at (A) 5 μm above the center of the cell. (B) Images taken at the center of the cell. (C) Images taken 5 μm below the center of the cell. The appearance of regions of fluorescence toward the center of the confocal images suggests that there is a degree of internalization of the SPNs into the cell. It also appears that the SPNs may adhere to the surface of the cell. The scale bar represents 10 μm.

As a preliminary study of the SPNs' viability in cell imaging, SH-SY5Y neuroblastoma cells were treated with MEH−PPV SPNs, as shown in Figure 4. The cells were treated for 18 h, and confocal microscopy was used to image them. The nucleus and actin were stained in order to indicate the cell periphery and cytoplasm. The SPNs were observed to cluster unilaterally in the perinuclear zone, suggesting they were contained within vesicles. If this were not the case, we would expect to observe a uniform distribution of the SPNs throughout the cytoplasm. The SPNs had no adverse affect on the cell or nuclear morphology during the study, suggesting they had little or no toxicological affect.

In a second imaging study, live HeLa cells were treated with MEH−PPV SPNs, as shown in Figure 5. In order to determine whether the nanoparticles were internalized into the cells, 40 optical sections were measured through individual cells in incremental steps of 500 nm from regions around the upper surface of the cell to the lower surface. The appearance of punctate regions of fluorescence not only around the periphery of the images but also around the center suggests that fluorescent nanoparticles are taken up and internalized by the cells. Fluorescence lifetime imaging (FLIM)[52] of polymer samples showed that the fluorescence lifetime was not easily resolvable using a system with an instrumental response function of ~250 ps. This is significantly shorter than the fluorescence lifetime of quantum dots in cells, which can be 2 orders of magnitude higher.[53] The cells did not appear to suffer any detrimental

(52) Festy, F.; M. Ameer-Beg, S.; Ng, T.; Suhling, K. *Mol. Biosyst.* **2007**, *3*, 381–391.

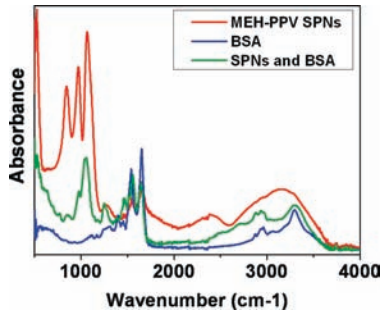

Figure 6. FTIR of free BSA, carboxylic acid functionalized MEH−PPV SPNs and SPN/BSA conjugates.

effects from the nanoparticles on the time scale of the incubation and imaging. The fluorescence images give clear evidence of the potential of these organic nanoparticles as fluorescent probes in both fixed and live cell imaging.

To be useful in a wide variety of imaging applications it is vital to be able to conjugate biomolecules to the nanoparticles. Carboxylic acid functionalized MEH−PPV SPNs were conjugated with BSA, a protein used extensively in assays, in order to demonstrate their potential for bioconjugation. A small proportion of the PEG_{2000}−PE was substituted with carboxylic acid functionalized PEG_{2000}−PE in order to functionalize the surface of the SPNs. Conjugation of the SPNs with BSA was performed by the formation of stable amide bonds between the carboxylic acid group and the primary amine groups of BSA. This was facilitated by the use of a sulfo-NHS and EDC reaction, with reference to published reports.[40] The hydrodynamic diameter of the carboxylic acid functionalized SPNs was measured before and after conjugation. A consistent increase in diameter was observed, between 5 and 10 nm. This appears consistent with the hydrodynamic diameter of BSA which is 6 nm at its maximum.[54]

To investigate whether BSA had conjugated to the nanoparticle, Fourier transform infrared (FTIR) spectroscopy was carried out. Spectra of the polymer nanoparticle, BSA, and BSA/polymer nanoparticle were obtained and compared, as shown in Figure 6. The major bends and stretches associated with BSA can be found at 1654 cm^{-1} (C═O stretch of the amide I band) 1543 cm^{-1} (N−H in plane bending and CN stretching, amide II band)[40] and were present in both the BSA and BSA/nanoparticle conjugate. A slight shift in the amide II band to 1560 cm^{-1} was observed, suggesting the BSA was linked to the particle. This has been seen previously when BSA was conjugated to semiconductor quantum dots.[40] In the polymer nanoparticle/BSA conjugate, a strong feature at 1064 cm^{-1} was also observed and was assigned to the ether stretch of the phospholipid when attached to BSA. This again has previously been observed in BSA/phospholipid conjugates of quantum dots.[40] Other notable features of the protein include the doublet N−H stretch in the amide A mode (3390 cm^{-1}) and the amide A′ mode (3082 cm^{-1}) that are also present in the nanoparticle/BSA conjugate. The nanoparticles alone do not exhibit this but show a large broad C−H feature as one might expect in MEH−PPV. This suggested that although the protein is linked to the particle, the overall integrity was maintained. In the nanoparticles without BSA, a strong feature was observed at 1072 cm^{-1} (an alkyl-oxygen stretch). This has been seen previously assigned as a shifted C−O−C ether stretch in the phospholipids or can be assigned to a shifted phenyl oxygen stretch in MEH−PPV.[55] Other strong features were 977 cm^{-1} (C−H bend in alkenes) and the 854 cm^{-1} (out-of-plane phenyl CH wag).

Conclusions

We have demonstrated the synthesis of phospholipid encapsulated conjugated polymer nanoparticles. MEH−PPV were successfully taken up and imaged inside SH-SY5Y neuroblastoma and live HeLa cells. Conjugation with BSA was also performed. The use of phospholipids for encapsulating hydrophobic materials was an intrinsic part of this simple and robust synthesis, rather than merely acting as a phase transfer agent. The emission wavelength of these SPNs was controlled by changing the type of conjugated polymer, and was tuned to emit across the visible spectrum. We have used only four types of conjugated polymer in this work, but an array of different types are commercially available, so it would be simple to tune the emission to a desired wavelength. Functionalized PEG−phospholipids are readily available which means various conjugation schemes could be used to functionalize these SPNs with biomolecules.

We envisage various uses for phospholipid encapsulated SPNs in biological fluorescence imaging, including live cell imaging and dynamics, and as biosensors. Of particular interest here is potential for use for in vivo fluorescence imaging. PEG−phospholipids bestow favorable biocompatibility properties upon the nanoparticles they encapsulate as they are nontoxic and exhibit excellent colloidal stability in water. They also increase circulation lifetime in vivo, which is an extremely important factor. However, even though PEG−phospholipid encapsulation increases biocompatibility, the use of toxic nanoparticle cores such as quantum dots would still be a concern. We suggest that the use of relatively benign conjugated polymers offers an excellent alternative for this type of work.

Acknowledgment. We acknowledge KCL for a studentship (P.H.) and KCL Business for funding (M.G., P.H.). We also thank the UK's Medical Research Council for funding K.S.'s research.

JA1002179

(53) Grecco, H. E.; Lidke, K. A.; Heintzmann, R.; Lidke, D. S.; Spagnuolo, C.; Martinez, O. E.; Jares-Erijman, E. A.; Jovin, T. M. *Microsc. Res. Tech.* **2004**, *65*, 169–179.
(54) Slayter, E. M. *J. Mol. Biol.* **1965**, *14*, 443–452, IN411−IN414.
(55) Yang, S.-H.; Wu, C.-C.; Lee, C.-F.; Liu, M.-H. *Displays* **2008**, *29*, 214–218.